

Collector factor in a solar chimney power plant: CFD analysis for the pilot plant in Manzanares

Erdem Cuce, Harun Sen

*Recep Tayyip Erdogan University
Department of Mechanical Engineering,
Rize, Turkey
Email: erdemcuce@gmail.com,
harun.sen6169@gmail.com*

Pinar Mert Cuce

*Recep Tayyip Erdogan University
Department of Architecture,
Rize, Turkey
Email: mertcuce@gmail.com*

Solar chimneys are popular systems for their simple structures and clean energy generation. Thanks to its semi-permeable structure, the collector, one of the system's basic elements, transfers solar radiation to the system. As a result of the heating of the system air under the collector by the solar radiation passing through the collector, it is directed to the high chimney in the collector centre. During the upward movement of the system air, it converts its energy into electricity via a turbine. Due to its large structure, estimating the amount of energy entering the collector system creates a great cost. The ideal size for the collector is therefore important. This study offers a recommendation for the ideal collector size for the pilot plant in Manzanares in terms of collector size and power output. While 59 kW power output is obtained with the system with a collector radius of 122 m in the reference case, it is observed that the power output increases by 78% when the collector radius is increased to 170 m and the collector area is doubled. The ratio of the ideal collector radius to the reference size for the pilot plant should be in the range of 1–1.5.

Keywords: solar chimney, solar chimney collector, ideal collector size

INTRODUCTION

The global need for energy is rising day by day depending on the human population. The use of fossil fuels is growing due to the increasing energy demand. This situation causes environmental pollution. The use of alternative energy sources is inevitable in order to minimise environmental pollution. One of the alternative energy sources is the sun, which can potentially be an alternative to fossil fuels. Solar energy can be used for different purposes and has been used by people since ancient times. Today, the areas of solar energy usage are constantly expanding. Researchers use the sun effectively outside of the purpose of indoor and

water heating with traditional methods. Solar cookers, fruit dryers, and natural ventilation are some of these uses [1–3]. In the mentioned methods, solar energy is used by absorbing directly. Apart from these, solar energy can be used to generate electricity directly or indirectly. Photovoltaic (PV) systems are popular systems that can produce electricity directly from the sun. PV systems, in which the incoming solar radiation is directly converted into electrical energy with the special materials they contain, have been widely used in recent years [4]. Systems that use solar energy indirectly are quite different from PV systems. Such systems are those that generate electricity on the condition of transferring solar energy to

air or a working fluid [5–6]. One of the systems working in this way is solar chimney power plants (SCPP). SCPP are systems with a simple structure and three basic elements: a turbine, a collector, and a chimney [7]. The solar radiation falling on the collector reaches the ground thanks to the translucency of the collector. At this moment, some of the solar radiation passes into the system air. Solar radiation reaching the ground also causes an increase in temperature on the ground. As the temperature of the system air increases, so does its speed. At the centre of the system collector is the high chimney. Due to its height, the chimney creates a continuous pressure difference and creates a vacuum effect at its entrance. The system air, whose temperature increases under the collector with the vacuum effect, is drawn upwards from the chimney inlet. In the meantime, the kinetic energy of the system air, whose temperature and speed increases with the turbine inside the chimney, is converted into electricity. Although the theoretical infrastructure of this simple system dates back to ancient times, it was first applied in the 1980s. The first plant with a chimney height of 194.6 m and a collector with a radius of 122 m is established in Manzanares, Spain [8]. The experimental measurements made at the facility in September, state that a power output of 50 kW is obtained at noon [9]. After the first facility, studies on the system increase

and researchers show great interest. Thanks to the high chimney in the SCPP structure, it can generate electricity by creating a continuous pressure difference [10]. In this way, it is an attractive system that can provide power output even when there is no sun. When the studies made after the first prototype were examined, the effect of the change in the geometric parameters of the system on the power output and efficiency were interpreted. In the following years, the researchers also analysed the effect of design parameters on the system performance. Today, when the studies on the system are examined, hybrid systems are emphasised. Hybrid systems focus on an SCPP to improve performance by integrating other renewable energy sources or waste energy. There are many geometric and design factors that affect the performance of the system. These are given in Table 1.

SCPP systems are disadvantageous compared to other systems due to their efficiency. However, the performance of these systems can be increased with some applications suggested by researchers in recent years. Designs such as the use of energy storage units on the ground, performance enhancement with waste heat or geothermal energy reinforcement, and additional power output with PV module integration have been popular in recent years. Some of the studies are given in Table 2.

Table 1. Effect of geometric, climatic, and design parameters on the system

References	The influence of climatic and geometric parameters	References	Design effects
[11–13]	Increasing the height of the chimney, which is the driving force of the system, positively affects the performance of the system. The chimney is the main element of the system.	[16–17]	It is effective in the performance of the system on the ground such as chimney and collector. Raising the floor towards the chimney inlet for the reference system increases the power output by 17%.
[14, 6]	Energy enters the system through the collector. For this reason, the increase in collector size directly increases the energy entering the system and contributes to the increase in performance. However, this situation comes to an end at some point.	[18–19]	A certain collector slope has a positive effect on the performance of the system. After a point, this effect turns negative.
[7, 15]	Initial temperature and solar radiation intensity are effective on the system. While solar radiation intensity has a positive effect on performance, the opposite is true for an increase in the starting temperature.	[19–21]	Divergent chimney design increases the performance of the system, so much so that the power output for the pilot plant can exceed two times with the ideal divergence angle.

Table 2. Effect of the energy storage unit and hybrid systems on SCPP

References	Energy storage unit	References	Hybrid systems
[22–23]	The use of soil or different materials on the ground for the purpose of energy storage allows power output outside the sun hours.	[26–27]	SCPP systems are large-scale. Adding PV modules to certain parts of the system can allow more power output. In addition, thanks to the airflow in the system, the PV modules can be cooled and their efficiency can be increased. Efficiency can reach ideal levels with the hybrid system designed in this way.
[24–25]	Water can be used for energy storage on the ground. Although this reduces the power output during daylight hours, it can allow for 24-hour power output.	[28–30]	SCPP systems can be used for many different purposes. One of them is to obtain clean water from seawater. More power output is claimed with this hybrid design.

Researchers have conducted different studies on SCPP systems. Although many parameters have been studied many times, there are many points that are not clear enough. Unlike traditional solar energy systems, SCPP systems can also output power during the hours when the sun is not present. This aspect differs from other systems. This study deals with the collector, which is one of the basic elements of the system. The size of the collector where the energy is transferred to the system is the focus of the study. First, the effect of the change in the collector size on the system for the pilot plant is evaluated.

A cost-optimal point is then sought for the collector size.

METHODS

In this study, the effect of the collector size in SCPP systems is analysed. While performing the analysis, the pilot plant dimensions are taken as a basis. The general view of the semi-transparent collector, where the solar energy is transferred to the system, the turbine that converts the kinetic energy of the air into electricity, and the system is given in Fig. 1.

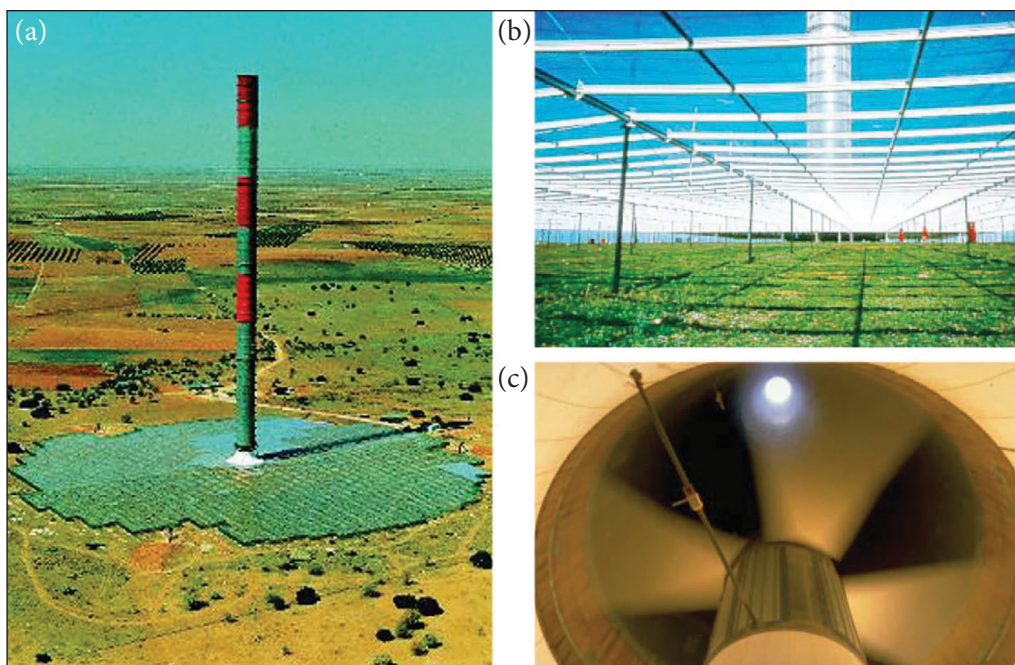


Fig. 1. An overview of the pilot plant in Manzanares, Spain (a); collector (b), and turbine (c) [8]

The data of the dimensions of the pilot plant and the geometric details of the computational fluid dynamics (CFD) model are given in Table 3. During the study, the diameter of the chimney outlet is 10.16 m and the collector radius is 122 m as a reference. Then, the collector radius is changed from 24.4 to 220 m in order to interpret the effect of the change of the collector area on the system. Although the solar radiation coming to the system reaches the ground, the experimental data shows that the temperature remains constant from 0.5 m below the ground [9]. In the light of the experimental data, 0.5 m soil thickness is considered ideal for the study. The student version of ANSYS engineering software was used in the study for CFD modelling and analysis. The model, the mesh image, and the system diagram for different collector sizes are given in Fig. 2. In the study, 90° symmetrical model

Table 3. Details of the geometric data of the study [8]

Geometric parameter	Value (m)
Chimney height	194.6
Chimney radius	10.16
Collector radius	122
Collector radius variation range	24.4–220
Collector height	1.85
Energy storage unit thickness	2

was used in terms of economy. In the analysis, the reference geometry was followed first. Then, only the collector radius was changed, keeping the climatic and geometric parameters constant.

The flow in the system is considered continuous and constant throughout the analysis. Climatic conditions remain unchanged in all analyses. Continuity, momentum and energy equations given below are solved coupled [5]:

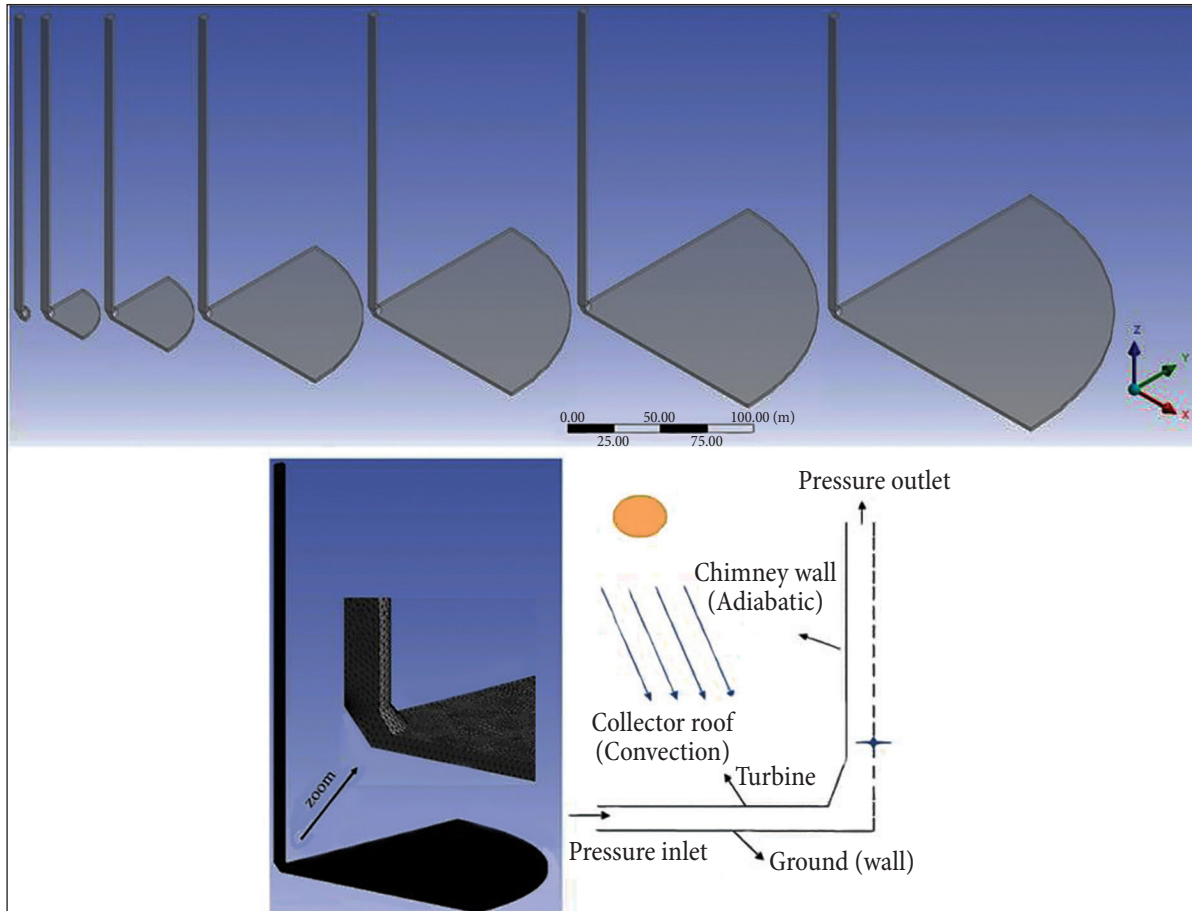


Fig. 2. Visuals of 3D CFD model, mesh, and boundary conditions

- Continuity equation

$$\frac{\partial(\rho u)}{\partial x} + \frac{\partial(\rho v)}{\partial y} + \frac{\partial(\rho w)}{\partial z} = 0. \quad (1)$$

- Momentum equation

$$\begin{aligned} & \frac{\partial(\rho uu)}{\partial x} + \frac{\partial(\rho uv)}{\partial y} + \frac{\partial(\rho uw)}{\partial z} \\ &= \frac{-\partial p}{\partial x} + \mu \left(\frac{\partial^2 u}{\partial x^2} + \frac{\partial^2 u}{\partial y^2} + \frac{\partial^2 u}{\partial z^2} \right); \\ & \frac{\partial(\rho vu)}{\partial x} + \frac{\partial(\rho vv)}{\partial y} + \frac{\partial(\rho vw)}{\partial z} \\ &= \frac{-\partial p}{\partial y} + \mu \left(\frac{\partial^2 v}{\partial x^2} + \frac{\partial^2 v}{\partial y^2} + \frac{\partial^2 v}{\partial z^2} \right); \end{aligned} \quad (2)$$

$$\begin{aligned} & \frac{\partial(\rho wu)}{\partial x} + \frac{\partial(\rho wv)}{\partial y} + \frac{\partial(\rho ww)}{\partial z} \\ &= \frac{-\partial p}{\partial z} + \mu \left(\frac{\partial^2 w}{\partial x^2} + \frac{\partial^2 w}{\partial y^2} + \frac{\partial^2 w}{\partial z^2} \right) + \rho g \beta (T - T_a). \end{aligned}$$

- Energy equation

$$\begin{aligned} & \frac{\partial(\rho cuT)}{\partial x} + \frac{\partial(\rho cvT)}{\partial y} + \frac{\partial(\rho cwT)}{\partial z} \\ &= \lambda \left(\frac{\partial^2 T}{\partial x^2} + \frac{\partial^2 T}{\partial y^2} + \frac{\partial^2 T}{\partial z^2} \right). \end{aligned} \quad (3)$$

Boundary conditions are important in analysis. Details are given in Fig. 2. For flow characteristics, turbulence is applied based on the literature [21]. The Boussinesq approximation for density is adopted as the buoyancy effects are significant. The power calculation of SCPP has

been done in different ways in the literature. In this study, the power output is calculated from the volumetric flow Q , turbine efficiency η_t , and turbine pressure drop ΔP_t , by the following equation [5]:

$$P_o = Q \times \eta_t \times \Delta P_t. \quad (4)$$

The turbine pressure drop can be calculated from the mean pressure difference at the turbine location as follows:

$$\Delta P_t = \frac{2}{3} \times P_t. \quad (5)$$

In the equation, P_t represents the average pressure difference at the turbine position and is obtained from the CFD results. The coefficient of 2/3 is taken according to the results obtained from the experimental data in the literature [9]. The study is based on the local latitude and longitude degrees of the pilot plant. In addition, solar ray tracing algorithm is used as a radiation model to evaluate real climatic conditions. The flow in the system is considered turbulent, and the RNG k - ϵ turbulence model is applied to the model [21]. The convergence criterion is taken as 10^{-6} . The properties and details of the materials used in the CFD study are given in Table 4.

RESULTS

Network-independent solution is extremely important in CFD studies. For this reason, in the study carried out, a network-independent solution is obtained first. When examined in detail in Table 5, the number of cells 379420 is considered suitable for the solution.

Table 4. Materials used in CFD and their properties [31]

Materials and properties	Chimney	Glass	Ground
Density (kg/m ³)	2100	2700	1900
Specific heat capacity (J/kg·K)	880	840	2200
Thermal conductivity (W/m·K)	1.4	0.78	0.8

Table 5. Mesh independence study

Cell count	V_{\max} (m/s)	P_o (kW)	% change V_{\max}	% change power
254761	15.31	62.27	–	–
379420	15.28	59	0.19	5.25
425853	15.32	59.35	0.26	0.59

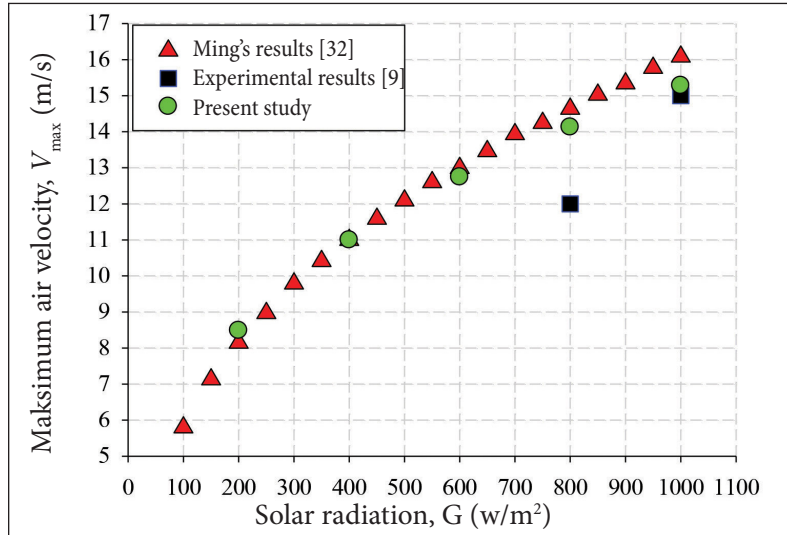


Fig. 3. Experimental results and comparison with literature to validate the CFD model

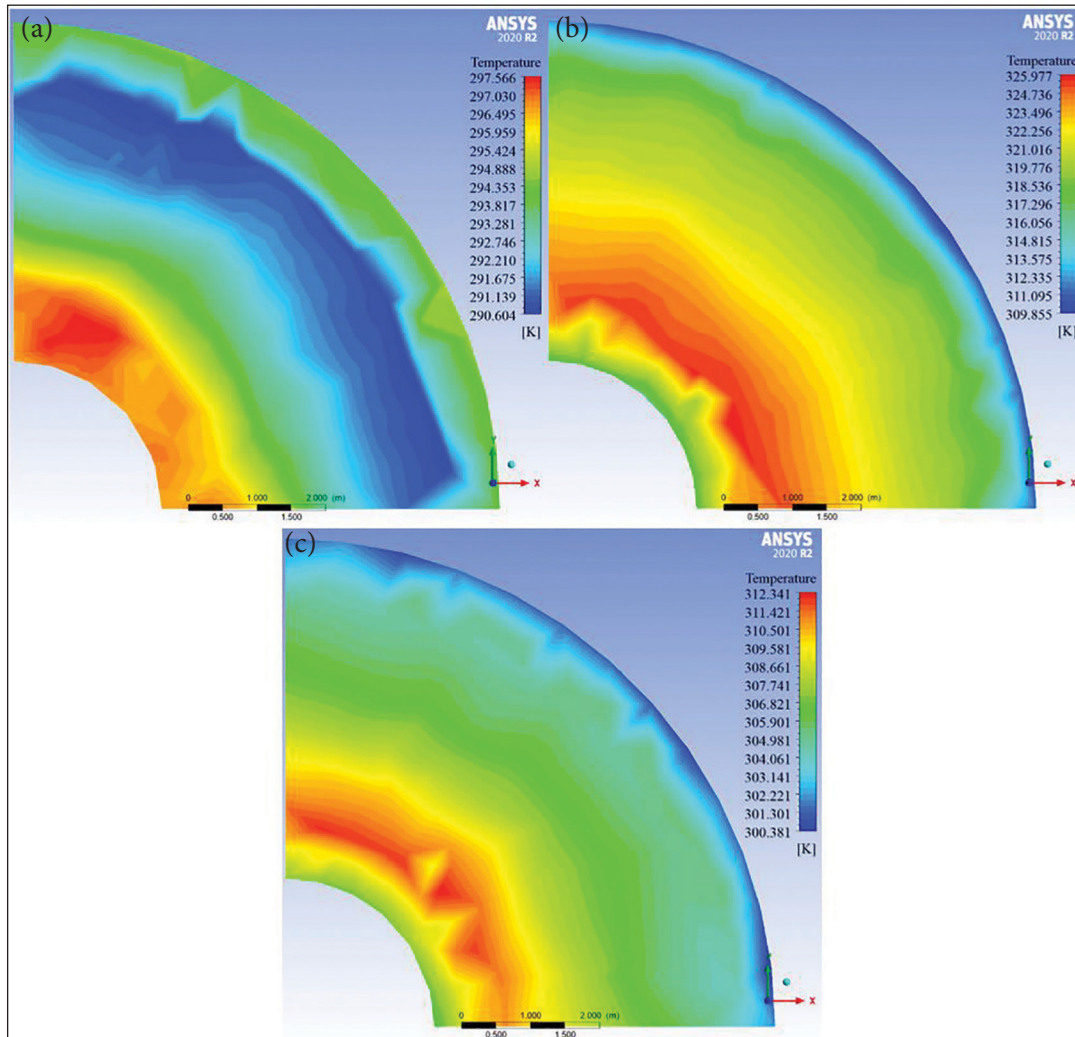


Fig. 4. Temperature distribution at the collector outlet: (A) 24.4 m collector radius, (B) 220 m collector radius, and (C) reference state (122 m collector radius)

Another criterion for the usability of the model is the experimental data. In the literature, the experimental data of the pilot plant and the results obtained from the study are compared. The results obtained from the model and the experimental data are consistent [32]. The graph of the comparison with the literature data and experimental data is given in Fig. 3. The maximum airflow velocity in CFD results for 1000 W/m^2 constant irradiation intensity and 290 K ambient temperature is 15.28 m/s . In the same climatic conditions, the experimental data show that the air flow rate is 15 m/s and is consistent with the study [9].

Increasing the collector radius directly increases the collector size. This means more energy transferred to the system. As a result, an increase in the performance of the system is expected. The reason for this is the expectation of a greater temperature difference and speed increase in the system air beneath the collector. Similarly, solar radiation reaches the ground through the semi-transparent collector and causes a temperature rise there as well. This temperature increases on the ground and the stored energy pass into the system air during the hours when the sun is absent or insufficient, resulting in an increase in performance [33–34]. The temperature distributions at the collector output for different collector radius are given in Fig. 4.

$X_{\text{coll} 1}$ is taken for the collector radius 122 m in the reference case. The power outputs are then calculated for the collector radius from 24.4 to 220 m . The power output increases with increasing X_{coll} , but tends to converge after a certain point. Details are given in Fig. 5. Increasing the collector radius increases the power output while increasing the cost. In this case, the maximum power to be obtained from the system in optimum dimensions for the ideal collector radius becomes important. It can be seen from the graph that the power output for the pilot plant in Manzanares increases continuously for the 146.6 – 183 m range of the collector radius. Increasing the collector radius beyond 183 m increases the power output of the system less than expected. Therefore, the 1 – 1.5 range can be taken as the ideal range for X_{coll} .

CONCLUSIONS

SCPP systems can also generate power during non-sun hours. In this respect, they differ from other solar energy systems. This study presents the range where the collector radius is optimal for the reference geometry for the pilot plant in Manzanares. RNG k-e turbulence model and sun ray tracing algorithm are used in the analysis made with the 3D CFD model. New solutions are taken with the model validated by experimental data

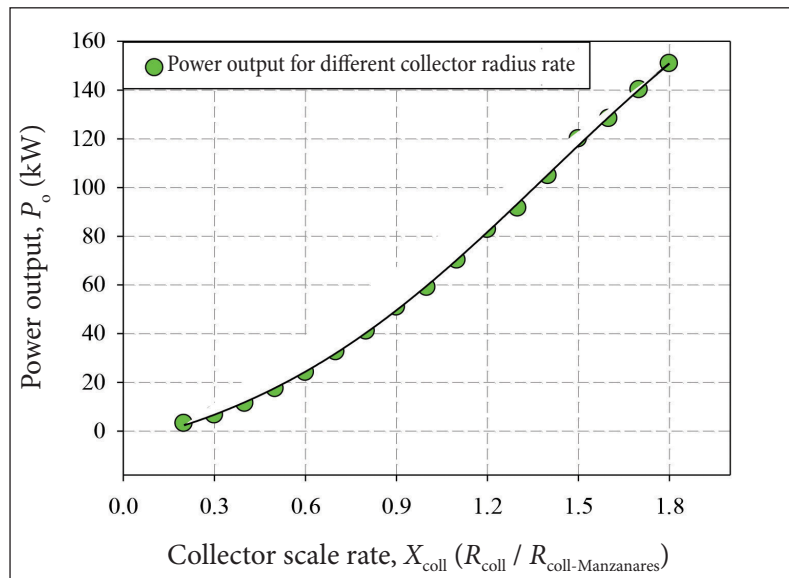


Fig. 5. Power output for different collector scale rates

and the literature. The ideal power output range is determined by changing the collector radius between 24.4 and 220 m. The results obtained from the study can be given as follows:

- The solar ray tracing algorithm for modelling solar radiation is suitable for SSCP systems. In addition, the RNG k-e model is suitable for modelling turbulence in the system.
- Increasing the collector radius improves system performance.
- Increasing the collector radius causes a greater temperature rise in the system air.
- With 1000 W/m² solar radiation and 290 K ambient temperature, the pilot plant system yields a power output of 59 kW.
- The air flow rate, which is 15 m/s in experimental measurements, is found as 1 000 W/m² solar radiation and 15.28 m/s at 290 K.
- The power output increases by 78% when the collector area is doubled. This indicates that the rate of increase in the power output is not proportional to the collector area.
- The ideal collector radius ratio for the pilot plant is 1–1.5. Above this value, the increase in the power output continues to decrease.
- The study shows that the collector size is critical to the system. For this reason, the collector size should be determined depending on the height of the chimney for the system to be installed.

Received 30 May 2022

Accepted 14 November 2022

References

1. Cuce P. M., Kolayli S., Cuce E. Enhanced performance figures of solar cookers through latent heat storage and low-cost booster reflectors. *International Journal of Low-Carbon Technologies*. 2020. Vol. 15. No. 3. P. 427–433. doi: 10.1093/ijlct/ctz079.
2. Afriyie J. K., Nazha M. A., Rajakaruna H., Forson F. K. Experimental investigations of a chimney-dependent solar crop dryer. *Renewable Energy*. 2009. Vol. 34. No. 1. P. 217–222. doi: 10.1016/j.renene.2008.04.010.
3. Maghrabie H. M., Abdelkareem M. A., Elsaid K., Sayed E. T., Radwan A., Rezk H., Wilberforce T., Abo-Khalil A. G., Olabi A. G. A review of solar chimney for natural ventilation of residential and non-residential buildings. *Sustainable Energy Technologies and Assessments*. 2022. Vol. 52. ID 102082. doi: 10.1016/j.seta.2022.102082.
4. Cuce P. M., Saxena A., Cuce E., Riffat S. Applications of solar PV tree systems with different design aspects and performance assessment. *International Journal of Low-Carbon Technologies*. 2022. Vol. 17. P. 266–278. doi: 10.1093/ijlct/ctac004.
5. Cuce P. M., Sen H., Cuce E. Impact of Tower Diameter on Power Output in Solar Chimney Power Plants. *Gazi Mühendislik Bilimleri Dergisi*. 2021. Vol. 7. No. 3. P. 253–263. doi: 10.30855/gmbd.2021.03.08.
6. Sen H., Cuce A. P. M., Cuce E. Impacts of Collector Radius and Height on Performance Parameters of Solar Chimney Power Plants: A Case Study for Manzanares, Spain. *Recep Tayyip Erdogan University Journal of Science and Engineering*. 2021. Vol. 2. No. 2. P. 83–104. doi: 10.53501/rteufemud.1017909.
7. Cuce E., Cuce P. M., Sen H. A thorough performance assessment of solar chimney power plants: Case study for Manzanares. *Cleaner Engineering and Technology*. 2020. Vol. 1. ID 100026. doi: 10.1016/j.clet.2020.100026.
8. Zhou X., Wang F., Ochieng R. M. A review of solar chimney power technology. *Renewable and Sustainable Energy Reviews*. 2010. Vol. 14. No. 8. P. 2315–2338. doi: 10.1016/j.rser.2010.04.018.
9. Haaf W. Solar chimneys: Part II: preliminary test results from the Manzanares pilot plant. *International Journal of Sustainable Energy*. 1984. Vol. 2. No. 2. P. 141–161. doi: 10.1080/01425918408909921.
10. Sen H., Cuce E. Dynamic pressure distributions in solar chimney power plants: A numerical research for the pilot plant in Manzanares, Spain. *WSSET Newsletter*. 2020. Vol. 12. No. 1. P. 2.
11. Sangi R. Performance evaluation of solar chimney power plants in Iran. *Renewable and Sustainable Energy Reviews*. 2012. Vol. 16. No. 1. P. 704–710. doi: 10.1016/j.rser.2011.08.035
12. Li J. Y., Guo P. H., Wang Y. Effects of collector radius and chimney height on power output of a solar chimney power plant with turbines.

- Renewable Energy*. 2012. Vol. 47. P. 21–28. doi: 10.1016/j.renene.2012.03.018.
13. Cuce E., Sen H., Cuce P. M. Numerical performance modelling of solar chimney power plants: Influence of chimney height for a pilot plant in Manzanares, Spain. *Sustainable Energy Technologies and Assessments*. 2020. Vol. 39. ID 100704. doi: 10.1016/j.seta.2020.100704.
 14. Toghraie D., Karami A., Afrand M., Karimipour A. Effects of geometric parameters on the performance of solar chimney power plants. *Energy*. 2018. Vol. 162. P. 1052–1061. doi: 10.1016/j.energy.2018.08.086.
 15. Larbi S., Bouhdjar A., Chergui T. Performance analysis of a solar chimney power plant in the southwestern region of Algeria. *Renewable and Sustainable Energy Reviews*. 2010. Vol. 14. No. 1. P. 470–477. doi: 10.1016/j.rser.2009.07.031.
 16. Cuce P. M., Cuce E., Sen H. Improving electricity production in solar chimney power plants with sloping ground design: an extensive CFD research. *Journal of Solar Energy Research Updates*. 2020. Vol. 7. No. 1. P. 122–131. doi: 10.31875/2410-2199.2020.07.10.
 17. Cuce E., Cuce P. M., Sen H., Sudhakar K., Bernardi U., Serencam U. Impacts of Ground Slope on Main Performance Figures of Solar Chimney Power Plants: A Comprehensive CFD Research with Experimental Validation. *International Journal of Photoenergy*. 2021. ID 6612222. doi: 10.1155/2021/6612222.
 18. Cottam P. J., Duffour P., Lindstrand P., Fromme P. Effect of canopy profile on solar thermal chimney performance. *Solar Energy*. 2016. Vol. 129. P. 286–296. doi: 10.1016/j.solener.2016.01.052.
 19. Hassan A., Ali M., Waqas A. Numerical investigation on performance of solar chimney power plant by varying collector slope and chimney diverging angle. *Energy*. 2018. Vol. 142. P. 411–425. doi: 10.1016/j.energy.2017.10.047.
 20. Cuce E., Saxena A., Cuce P. M., Sen H., Guo S., Sudhakar K. Performance assessment of solar chimney power plants with the impacts of divergent and convergent chimney geometry. *International Journal of Low-Carbon Technologies*. 2021. Vol. 16. No. 3. P. 704–714. doi: 10.1093/ijlct/ctaa097.
 21. Hu S., Leung D. Y., Chen M. Z. Effect of divergent chimneys on the performance of a solar chimney power plant. *Energy Procedia*. 2017. Vol. 105. P. 7–13. doi: 10.1016/j.egypro.2017.03.273.
 22. Cuce E., Saxena A., Cuce P. M., Sen H., Eroglu H., Selvanathan S. P., Sudhakar K., Hasanuzaman M. Performance assessment of solar chimney power plants with natural thermal energy storage materials on ground: CFD analysis with experimental validation. *International Journal of Low-Carbon Technologies*. 2022. Vol. 17. P. 752–759. doi: 10.1093/ijlct/ctac001.
 23. Guo P., Wang Y., Li J., Wang Y. Thermodynamic analysis of a solar chimney power plant system with soil heat storage. *Applied Thermal Engineering*. 2016. Vol. 100. P. 1076–1084. doi: 10.1016/j.applthermaleng.2016.03.008.
 24. Choi Y. J., Kam D. H., Park Y. W., Jeong Y. H. Development of analytical model for solar chimney power plant with and without water storage system. *Energy*. 2016. Vol. 112. P. 200–207. doi: 10.1016/j.energy.2016.06.023.
 25. Semai H., Bouhdjar A., Larbo S. Canopy slope effect on the performance of the solar chimney power plant. *International Journal of Green Energy*. 2017. Vol. 14. No. 3. P. 229–238. doi: 10.1080/15435075.2016.1253580.
 26. Rahbar K., Riasi A. Performance enhancement and optimization of solar chimney power plant integrated with transparent photovoltaic cells and desalination method. *Sustainable Cities and Society*. 2019. Vol. 46. ID 101441. doi: 10.1016/j.scs.2019.101441.
 27. Singh A. P., Kumar A., Singh O. P. Performance enhancement strategies of a hybrid solar chimney power plant integrated with photovoltaic panel. *Energy Conversion and Management*. 2020. Vol. 218. ID 113020. doi: 10.1016/j.enconman.2020.113020.
 28. Mendez C., Bicer Y. Integration of solar chimney with desalination for sustainable water production: A thermodynamic assessment. *Case Studies in Thermal Engineering*. 2020. Vol. 21. ID 100687. doi: /10.1016/j.csite.2020.100687.
 29. Zhou X., Xiao B., Liu W., Guo X., Yang J., Fan J. Comparison of classical solar chimney power system and combined solar chimney system for

- power generation and seawater desalination. *Desalination*. 2010. Vol. 250. No. 1. P. 249–256. doi: 10.1016/j.desal.2009.03.007.
30. Ming T., Gong T., de Richter R. K., Cai C., Sherif S. A. Numerical analysis of seawater desalination based on a solar chimney power plant. *Applied Energy*. 2017. Vol. 208. P. 1258–1273. doi: 10.1016/j.apenergy.2017.09.028.
31. Pandey M., Padhi B. N., Mishra I. Performance analysis of a waste heat recovery solar chimney for nocturnal use. *Engineering Science and Technology, an International Journal*. 2021. Vol. 24. No. 1. P. 1–10. doi: 10.1016/j.jestch.2020.11.009.
32. Tingzhen M., Wei L., Guoliang X. Analytical and numerical investigation of the solar chimney power plant systems. *International Journal of Energy Research*. 2006. Vol. 30. No. 11. P. 861–873. doi: 10.1002/er.1191.
33. Cuce E., Sen H. Solar chimney power plants from past to present: Performance parameters affecting system power output. *Euro Asia 7th International Congress on Applied Sciences, 21–22 August, 2020, Trabzon, Turkey*. P. 256–262.
34. Cuce E., Cuce P. M., Carlucci S., Sen H., Sudhakar K., Hasanuzzaman M., Daneshazarian R. Solar chimney power plants: a review of the concepts, designs and performances. *Sustainability*. 2022. Vol. 14. No. 3. ID. 1450. doi: 10.3390/su14031450.

Erdem Cuce, Harun Sen, Pinar Mert Cuce

**SAULĖS KAMINO ELEKTRINĖS KOLEKTORIAUS KOEFICIENTAS: MANSANARESO
BANDOMOSIOS JĖGAINĖS SKAIČIUOJAMOSIOS SKYSČIŲ DINAMIKOS (CFD) ANALIZĖ**